Supporting Information for

Highly Elastic Hydrated Cellulosic Materials with Durable Compressibility and Tunable Conductivity

Chaoji Chen[1a], Jianwei Song[1a], Jian Cheng[2a], Zhenqian Pang[2], Wentao Gan[1], Gegu Chen[1], Yudi Kuang[1], Hao Huang[2], Upamanyu Ray[2], Teng Li[2,*], Liangbing Hu[1,*]

1. Department of Materials Science and Engineering, University of Maryland, College Park, Maryland, 20742
2. Department of Mechanical Engineering, University of Maryland, College Park, Maryland, 20742

[*] Email: binghu@umd.edu, lit@umd.edu

[a] These authors contributed equally to this work.

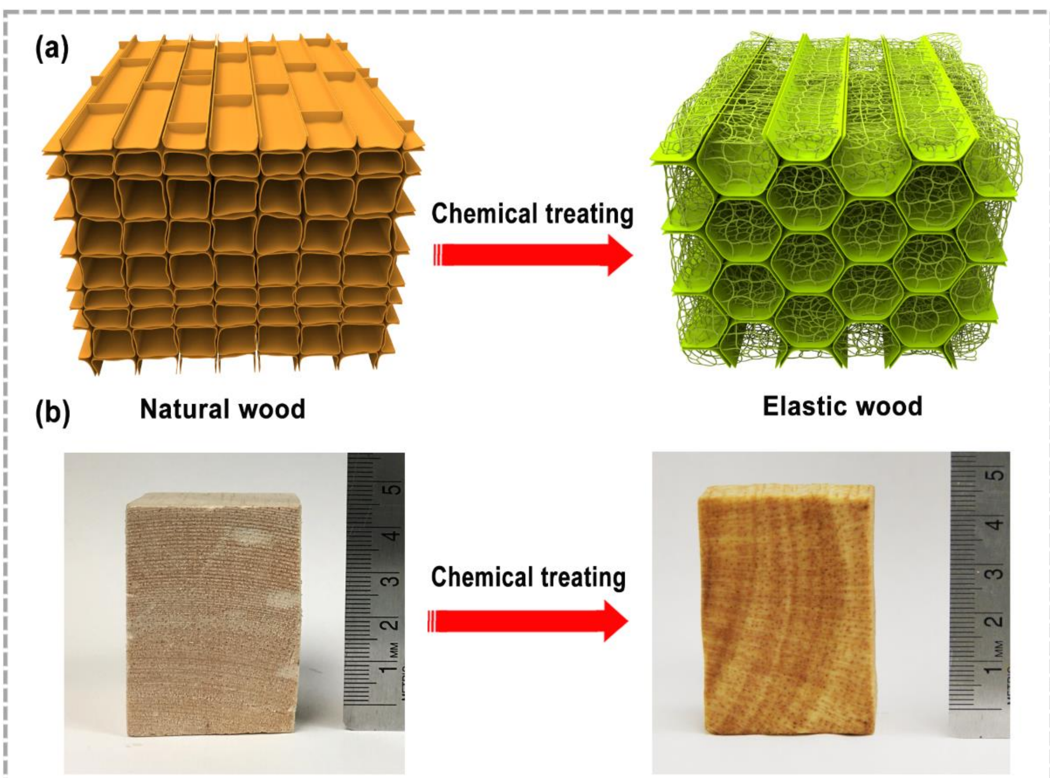

Figure S1. Graphical illustration (a) and photo images (b) of the natural wood (balsa) and elastic wood.

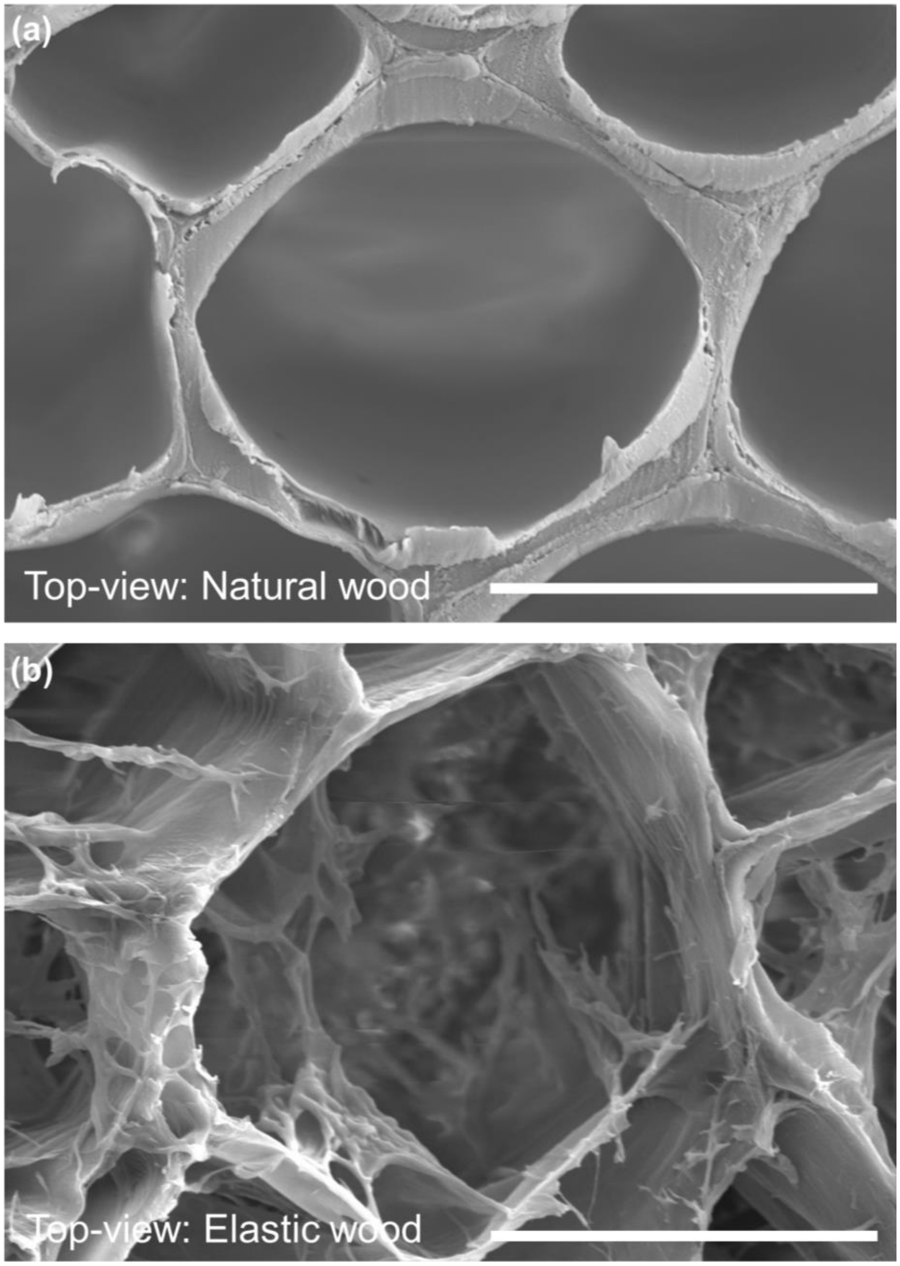

Figure S2. Magnified top-view SEM images of natural wood (a) and elastic wood (b). Scale bar: 30 μm. The result showed that the cell wall of balsa wood became thinner after chemical treatment. In addition, loose inner cellulose fibril network was formed.

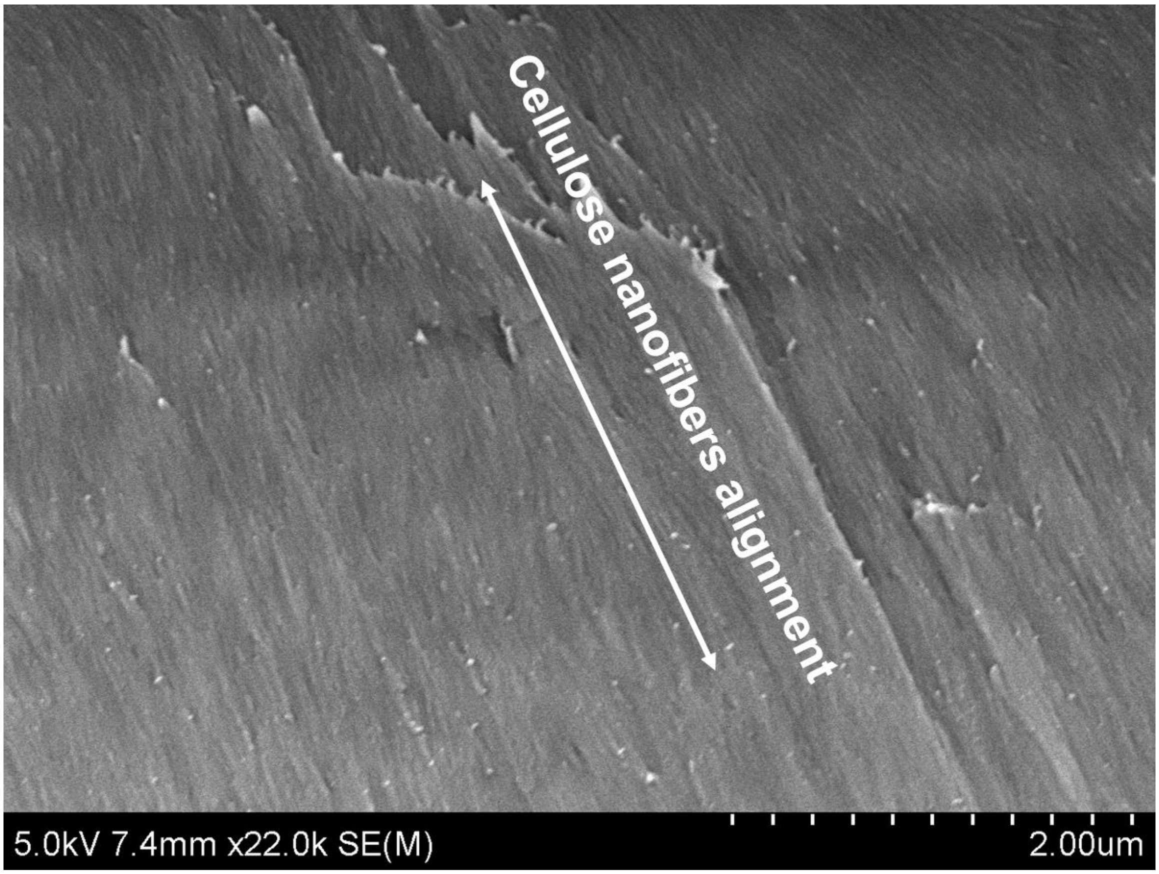

Figure S3. Magnified SEM image of the elastic wood showing aligned cellulose nanofibers.

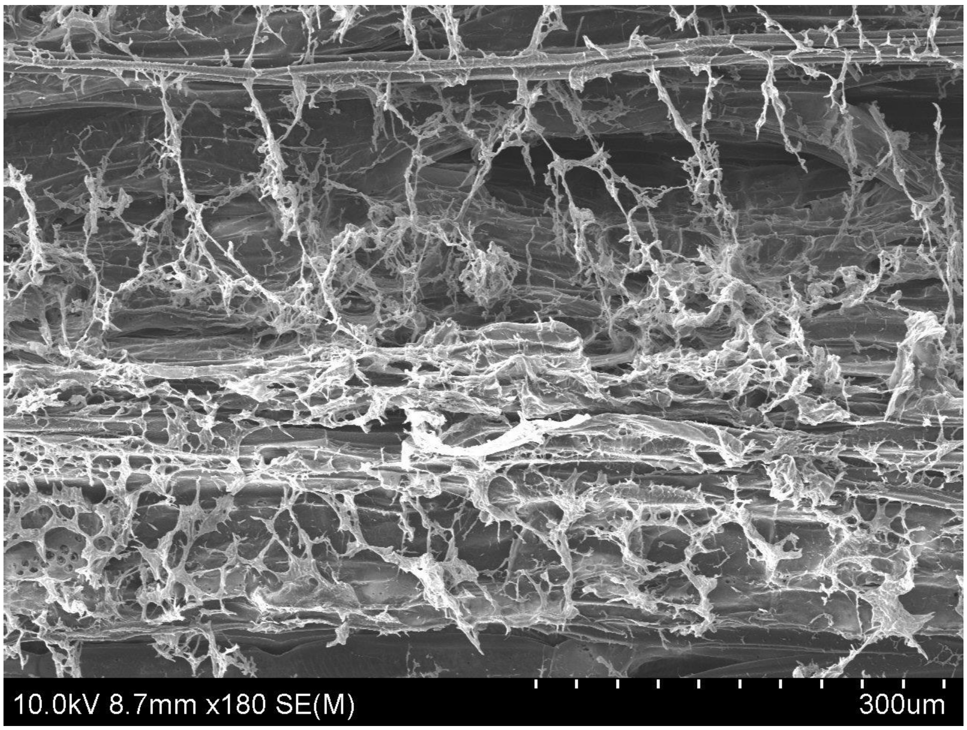

Figure S4. Magnified SEM image showing the cellulose fibril network inside the lumen of the elastic wood.

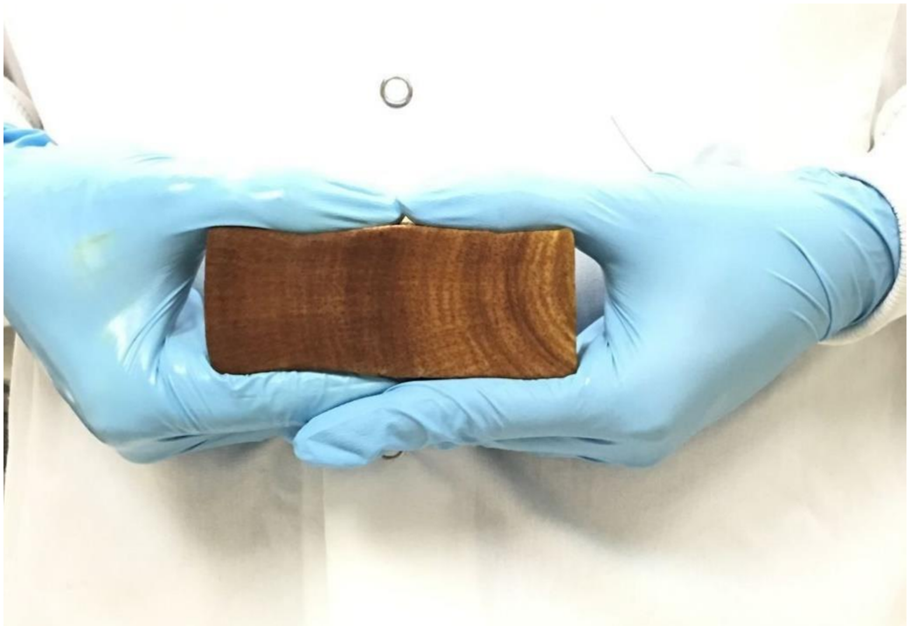

Figure S5. Photo image of a large-sized elastic wood.

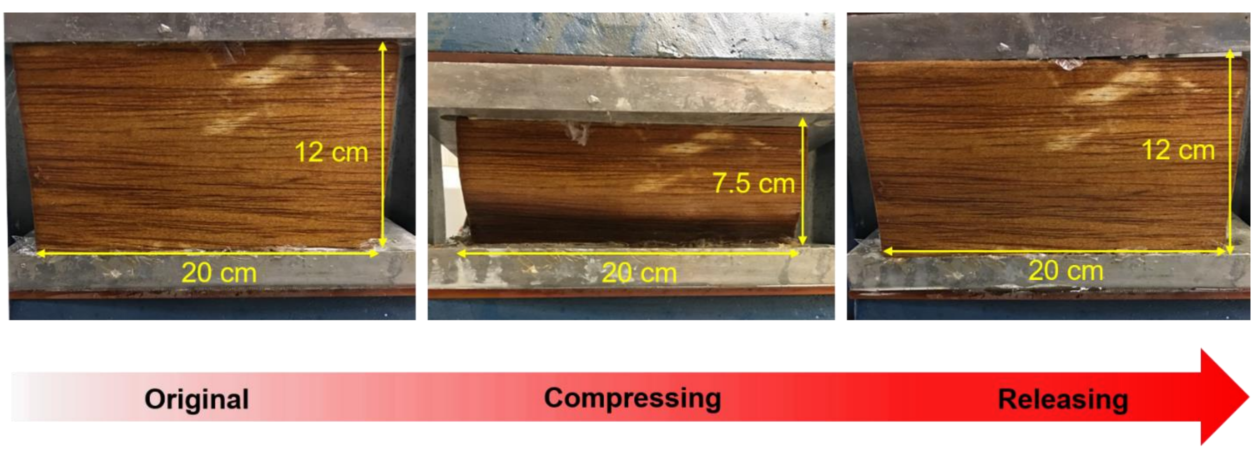

Figure S6. Compression and releasing of a large-sized elastic wood.

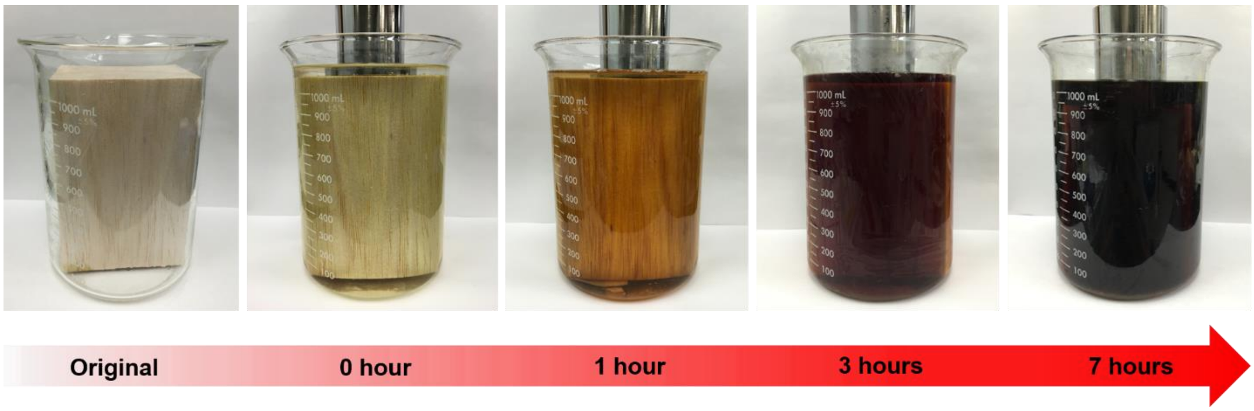

Figure S7. Color change during treating the wood samples.

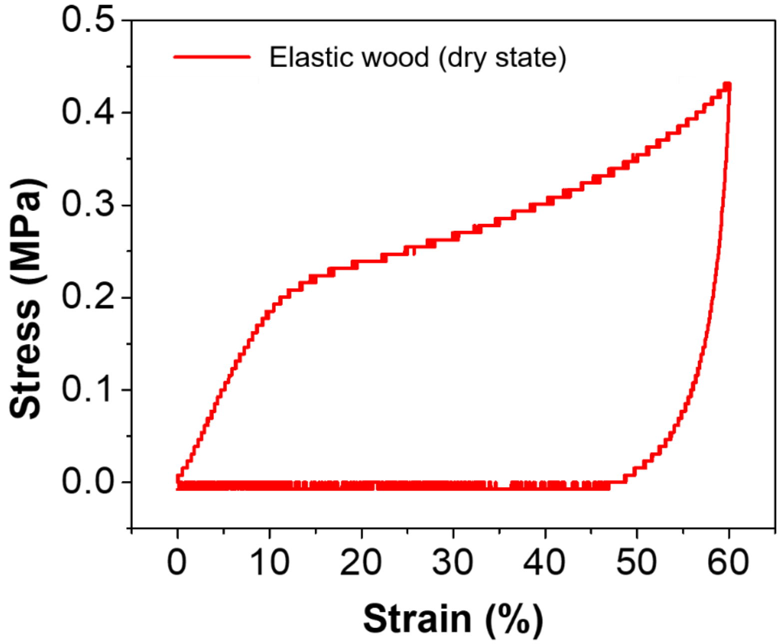

Figure S8. Compressive stress-strain curve of the elastic wood at dry state.

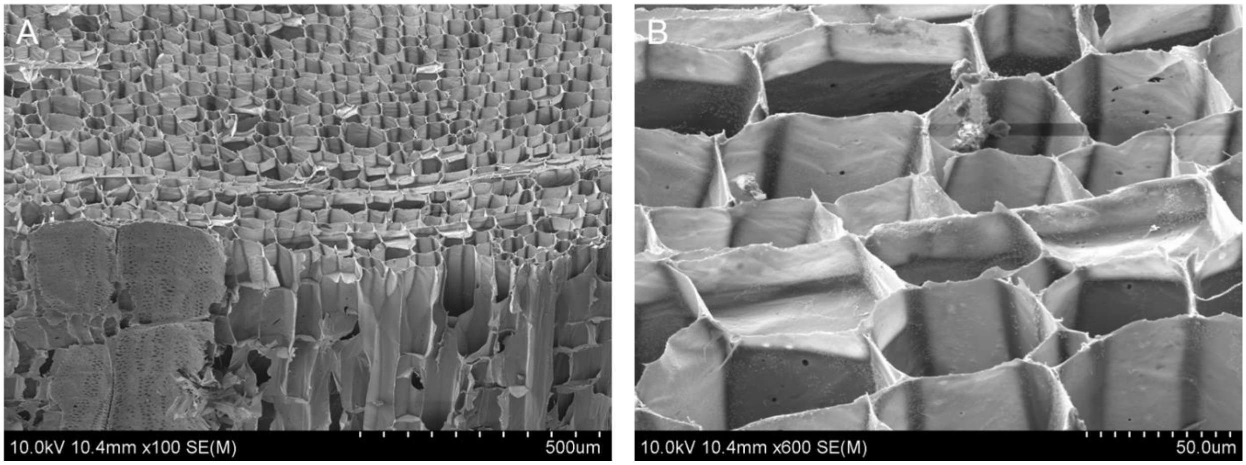

Figure S9. (a, b) SEM images of the completely delignified wood. The cell walls become much thinner than natural wood after completely delignification. In addition, no inner gel network is observed.

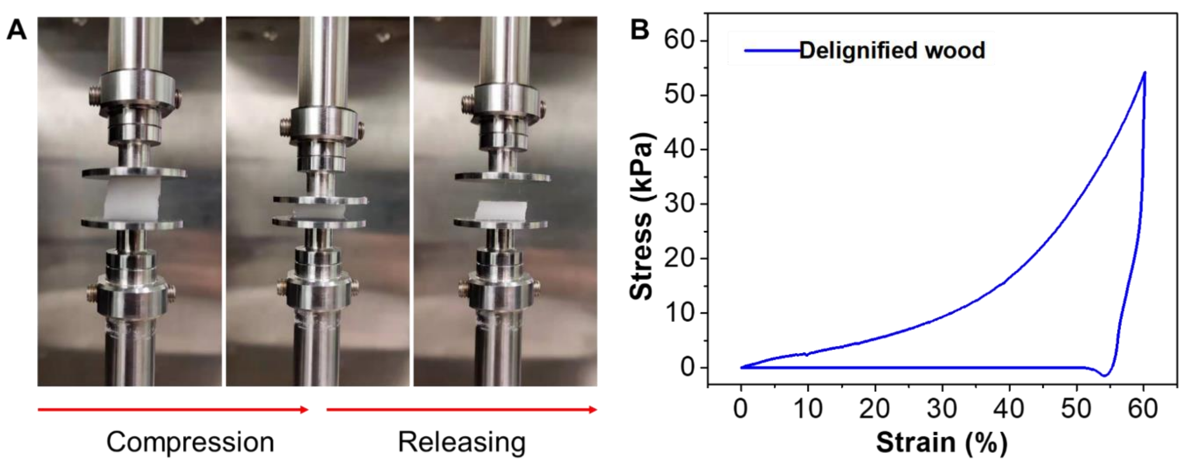

Figure S10. Compression test of the completely delignified wood: (a) photo images and (b) stress-strain curve. the delignified wood becomes less compressive with a large plastic deformation of 55% and low ultimate compressive stress of 55 kPa at 60% strain due to the nearly complete removal of lignin and hemicellulose.

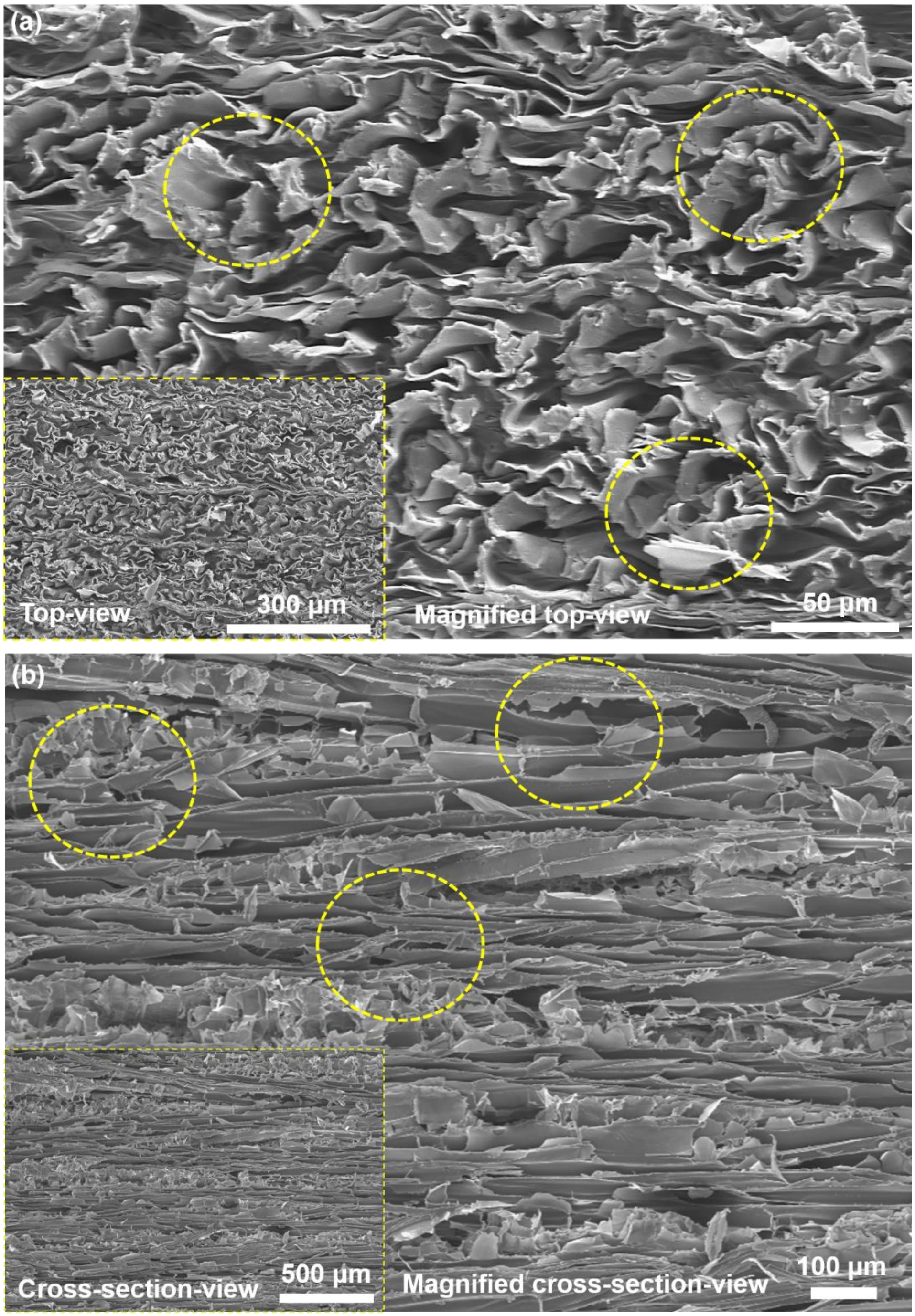

Figure S11. SEM image of the natural balsa wood after compressed: (a) top-view, (b) longitudinal-section-view.

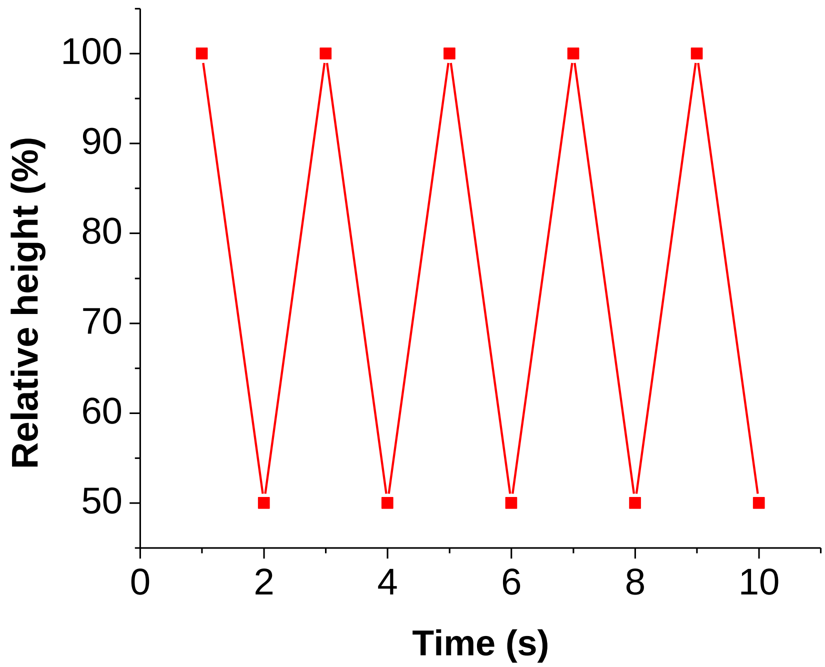

Figure S12. Relative height of the elastic wood as a function of time upon repeated compressing/releasing cycles. The elastic wood can quickly recover from a compression of 50% within a short time of 1 second.

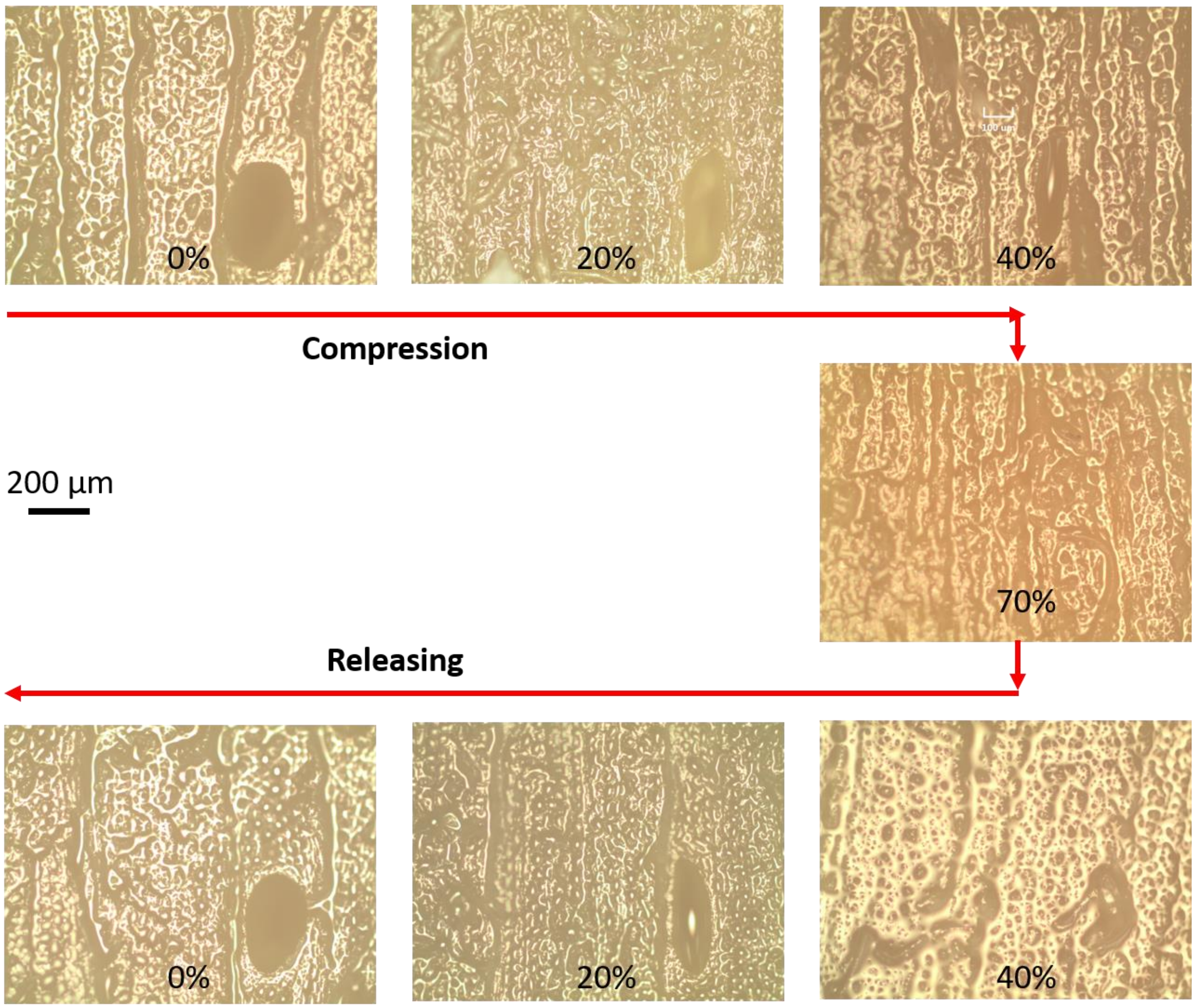

Figure S13. *Ex situ* observation of the morphological evolution of elastic wood (wet state) under compression/releasing cycle using optical microscopy. The pores (*e.g.*, lumina of vessels and fibres) were pressed to a smaller size during compression, which can reversibly recover to its original size and shapes after releasing the compression, indicating the excellent elastic compressibility of the elastic wood.

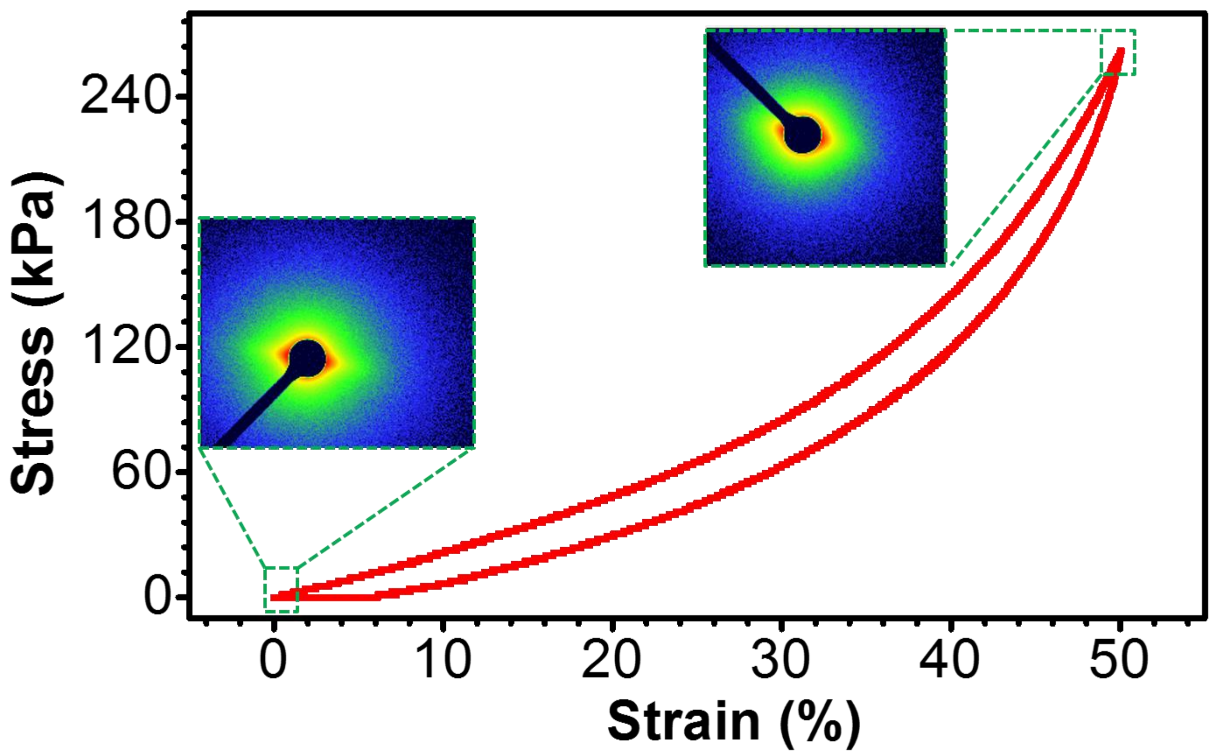

Figure S14. Compressive stress-strain curve of the elastic wood. Insets show the SAXS patterns of the original elastic wood and under 50% compressive strain.

Atomistic simulation

The full atomistic simulation using ReaxFF potential[1] implemented in the Large-Scale Atomic/Molecular Massively Parallel Simulator (Lammps)[2] simulation package is performed to determine the atomic interaction between fibrils and water. ReaxFF potential can be widely used to describe chemical bonds and weak interaction, such as hydrogen bonds and van der Walls force[3]. There are 16 cellulose chains around with hemicellulose and lignin units aligned as cubic arrangement (4×4) in our simulations. It has been confirmed that 4×4 chains are large enough to illustrate the interactions of the fibrils[4], due to the same functional groups. A Nose-Hoover thermostat is used to maintain the NPT and NVT ensembles at 300 K in the process of relaxing and compression, respectively. The timestep is set as 0.5 fs and the periodic boundary conditions are applied in both *x*-, *y*- and *z-directions* for all the models. All the calculations are relaxed using the conjugate gradient (CG) algorithm to minimize the total energy of the system until the total atomic forces are converged to less than 10^{-9} eV/Å. We first equilibrate the structures at room temperature (300 K) and external pressure with 0 Pa for 5 ps. In this process we can relax the models sufficiently and define the size of the models in *y-direction* as original (O) length ($L_{original}$). Considering the interaction between water and cellulose, the cellulose will be adhered tightly by water. Thus, the size of model with water which is about 60 Å *41 Å *30 Å is much smaller than that without water (72 Å *80 Å *80Å). The displacement loading applied to *y-direction* is indicated by green arrows in the end views of Figure 5. After compressing the models for 25 ps, we set the models in zero pressure environment for 25 ps to release the internal stress sufficiently. For visual clarity, we show the snapshot of section view of the cellulose molecular chains only (water molecules are not shown). The percentage (%) of compression (C) is calculated by ($L_{compressed}$ / $L_{original}$) *100, where $L_{compressed}$ is the compressed length of the models kept along *y-direction*. The percentage (%) of recovery (R) is calculated by ($L_{recovered}$ / $L_{original}$) *100, where $L_{recovered}$ represents recovered length of the model (along *y-direction*) after loading is released and the model is allowed to recover. The water content (wt%) is defined by ($M_{water}/M_{water+cellulose}$)*100, where the $M_{water+cellulose}$ is the total mass of model and M_{water} is the mass of water in the system. Comparing to the water content of elastic wood (65 wt%) [5], we calculated the model with the water content about 60 wt%.

FEM modeling details:

Given the large length-to-diameter ratio (over 1000) of the cellulose fibril bundles and their rather random distribution in the transverse cross-section, it is reasonable to describe the cellular wall as a transversely isotropic material. The thickness of the cellulose wall is taken to be 13.8% of the size of a single hexagon cell, which is 50 μm. And the following mechanical properties are used in the simulation: Young's modulus E = 70 GPa, Poisson's ratio v = 0.3, yield strength σ_Y = 600 MPa, post-yielding modulus E_2 = 9.5 GPa. The loading procedure is modeled as a quasi-static procedure. In this case, a mass scaling factor of 2 is used in the simulation to help the algorithm overcome the numerical singularity due to buckling instability and contact clattering. This numerical treatment is valid in the calculation and does not alter the result since the total kinetic energy in the model is less than 2% of the total energy associated with deformation and dissipation. A total number of 1798 linear plane-strain continuum elements are used in the finite element model. To capture the post-buckling deflection, it has been included in the structure a small extend (scaling factor 0.01 for the primary mode, 0.005 for the secondary and higher order) of geometry imperfection, which is derived from the linear buckling analysis. A quasi-static analysis step at a strain rate of 0.006/s is used to stabilize the high nonlinearity due to plasticity, buckling, and contact. In the elastic wood finite element model, the wall thickness is reduced by a factor of 33% in order to account for the chemical treatment.

To investigate the effects of the stiffness μ_0 on the compressive responses of the elastic wood, and to estimate the effective shear modulus of the interconnected cellulose fibrils, a series of cases with different values of μ_0/μ_s are shown in Figure S15. The stress-strain curve in absence of the wood gel is featured by a continuous competition between the softening effect caused by buckling and the overall structural stiffening due to contact. By comparing Figure S15a with S15b, it is concluded that even very compliant (μ_0/μ_s=0.001) wood gel filling between the walls is able to stabilize the compress response. However, two distinct stages can be identified on the stress-strain curve with μ_0/μ_s=0.001. This is because the stiffness μ_0 is too small. μ_0/μ_s=0.01 is suitable for the elastic wood in our study, as the stress-strain curve is in good agreement with the experiment. Lastly, μ_0/μ_s=0.1 is too high so that no cell wall collapse is observed. Therefore, it is concluded that the value of μ_0/μ_s is on the order of 0.01.

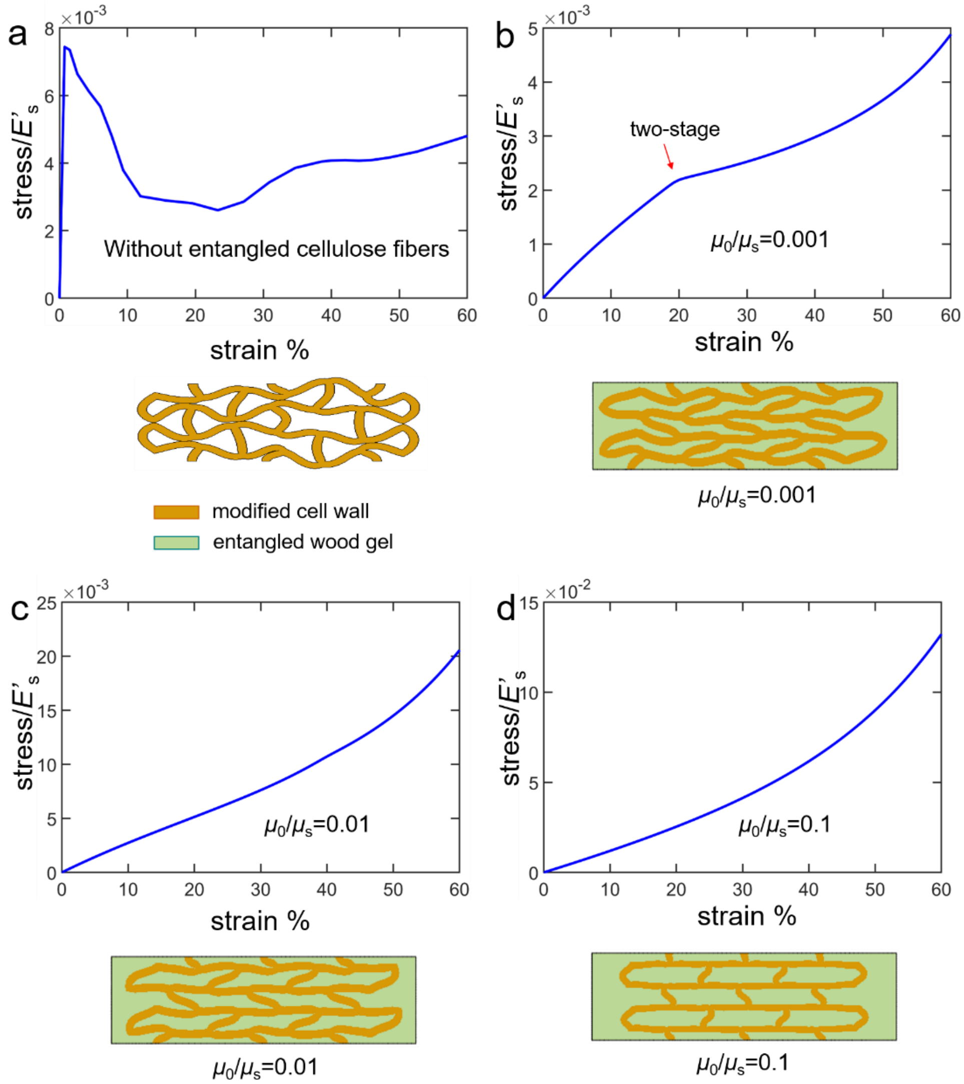

Figure S15. (a) Elastic wood without entangled cellulose fibrils. (b)~(d) Elastic wood with entangles cellulose fibrils of different stiffness (b) μ_0/μ_s=0.001, (c) μ_0/μ_s=0.01, (d) μ_0/μ_s=0.1, where μ_0 is the initial shear modulus of wood gel, and μ_s is the shear modulus of the modified wood cell wall. All the snapshots of the deformed elastic wood structures are taken at prescribed strain of 80%.

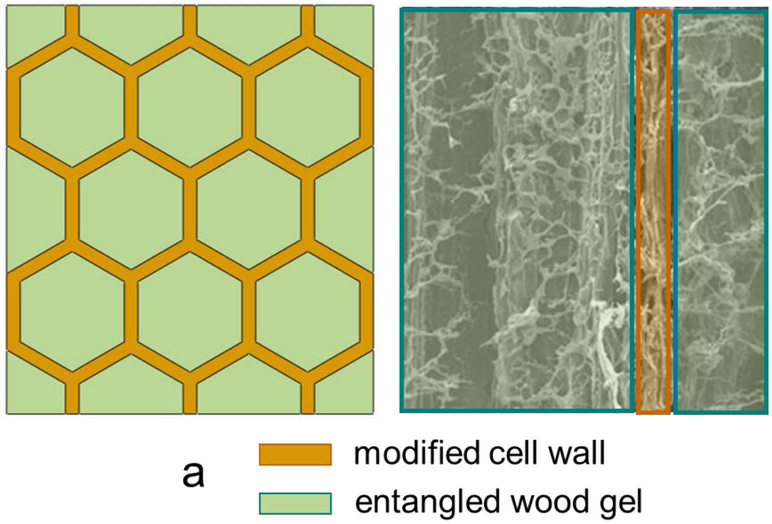

Figure S16. Structure of the elastic wood. The hexagonal cell walls are made of modified wood which is super rich in water. The cells are filled with entangled cellulose fibrils holding water content. The initial shear modulus ratio between the modified wood and the wood gel is 100:1.

Compositional analysis details:

Compositional analysis was performed to determine the contents of cellulose, hemicellulose and lignin. The "starting-point" is natural wood composition content. For natural wood, the yield is 100%, thus the normalized value of content is equal to the test value.

The elastic wood was prepared by cooking the dry natural wood in a mixture solution of Sodium Hydroxide (NaOH) and Sodium Sulfite (Na_2SO_3) at 100 °C for 3 to 7 hours (depending on the size of the wood blocks). The equation for the yield (Y) is

$$Y = [m_1/m_0]*100\% \qquad (1)$$

where m_1 is the weight of the elastic wood, m_0 is the weight of dry natural wood. After chemical treatment, the weight percentage of natural wood decreases from 100% to 78%.

Measurement of the cellulose, hemicellulose, and lignin content was carried out by the standard protocol used at the USDA Forest Products Lab (Madison, Wisconsin, USA) as described previously[5]. We normalized the test values of cellulose (or hemicellulose, or lignin) content to compare the evolutions from natural wood to elastic wood. The normalized value of content for cellulose, hemicellulose and lignin were calculated by:

$$C_{(normalization)} = [C_{(test)}*Y]*100\% \qquad (2)$$

where $C_{(test)}$ is the test value, Y is the yield, and C (normalization) is the normalized value. All the test and normalized values of cellulose, hemicellulose, and lignin for natural wood and elastic wood are summarized in Table S1.

Table S1. The chemical composition evolution from natural wood to elastic wood.

		Cellulose (%)	**Hemicellulose (%)**	**Lignin (%)**	**Others (%)**
Natural wood (Treated 0h)	Test value (After normalization)[a]	39.5	16	26	18.5
Elastic wood	Test value	48.1	14.5	24.9	12.5
	Yield	78.0%			
	After normalization	37.5 (48.1*78%)	11.3 (14.5*78%)	19.4 (24.9*78%)	9.75 (12.5*78%)

Note:
a. For natural wood, the yield is 100%, thus the normalized value of content is equal to the test value.

Captions of videos:

Movie S1: Repeated compression/releasing of the elastic wood block, demonstrating its excellent elasticity.

Movie S2: Repeated compression/releasing of the elastic wood ball.

Movie S3: Throwing and rebounding of the elastic wood ball.

Reference

1. Mattsson, T. R.; Lane, J. M. D.; Cochrane, K. R.; Desjarlais, M. P.; Thompson, A. P.; Pierce, F.; Grest, G. S., First-Principles and Classical Molecular Dynamics Simulation of Shocked Polymers. *Phys. Rev. B* **2010,** *81*, 054103.

2. Plimpton, S., Fast Parallel Algorithms for Short-Range Molecular Dynamics. *J. Comput. Phys.* **1995,** *117*, 1-19.

3. Zhu, H.; Zhu, S.; Jia, Z.; Parvinian, S.; Li, Y.; Vaaland, O.; Hu, L.; Li, T., Anomalous Scaling Law of Strength and Toughness of Cellulose Nanopaper. *PNAS* **2015,** *112*, 8971-8976.

4. Shishehbor, M.; Zavattieri, P. D., Effects of Interface Properties on the Mechanical Properties of Bio-Inspired Cellulose Nanocrystal (CNC)-Based Materials. *J. Mech. Phys. Solids* **2019,** *124*, 871-896.

5. Luo, X.; Gleisner, R.; Tian, S.; Negron, J.; Zhu, W.; Horn, E.; Pan, X.; Zhu, J., Evaluation of Mountain Beetle-Infested Lodgepole Pine for Cellulosic Ethanol Production by Sulfite Pretreatment to Overcome Recalcitrance of Lignocellulose. *Ind. Eng. Chem. Res.* **2010,** *49*, 8258-8266.